

Triangular antiferromagnet with nonmagnetic impurities

V. S. Maryasin and M. E. Zhitomirsky

*Service de Physique Statistique, Magnétisme et Supraconductivité,
UMR-E9001 CEA-INAC/UJF, 17 rue des Martyrs, 38054 Grenoble, France*

(Dated: March 14, 2019)

The effect of nonmagnetic impurities on the phase diagram of the classical Heisenberg antiferromagnet on a triangular lattice is investigated. We present analytical arguments confirmed by numerical calculations that at zero temperature vacancies stabilize a conical state providing an example of ‘order by quenched disorder’ effect. Competition between thermal fluctuations and the site disorder leads to a complicated H - T phase diagram, which is deduced from the classical Monte Carlo simulations for a representative vacancy concentration. For the XY triangular-lattice antiferromagnet with in-plane external field nonmagnetic impurities stabilize the fan-like spin structure. We also briefly discuss the effect of quantum fluctuations.

PACS numbers: 75.10.Hk, 75.10.Nr, 75.40.Mg, 75.50.Ee

Introduction.—Spin vacancies produced by substitution of nonmagnetic ions is a common form of disorder in magnetic solids. Nonmagnetic impurities are often used experimentally as a probe of local spin correlations [1, 2]. Accordingly, many theoretical works were devoted to investigation of magnetization patterns and spin textures around a single impurity in ordered, spin-liquid, and quantum-critical antiferromagnets [3–14]. Scaling from a single vacancy to a more realistic situation of small but finite concentration of impurities is straightforward for simple collinear antiferromagnets. In the case of frustrated magnets with a ground-state degeneracy the problem of collective impurity behavior becomes much more nontrivial due to a possible “order by quenched disorder” effect [15–17].

In this Letter we consider the triangular-lattice antiferromagnets (TAFMs), which attracted a lot of interest in the past as a paradigmatic example of geometrical frustration [18–22] and also due to their intrinsic multiferroicity [23, 24]. A single nonmagnetic impurity embedded into the TAFM was investigated by Wollny *et al.* [11]. They found that a fractional magnetic moment collinear with the ‘missing’ spin is formed around a vacancy site. In magnetic field the clean classical TAFM exhibits an ‘accidental’ degeneracy consisting in an arbitrary orientation of the spin plane with respect to the field direction [19, 20]. Hence, the impurity moment may stabilize the same coplanar magnetic structures, Fig. 1(a)–(c), that are also favored by thermal and quantum fluctuations—the scenario advocated in [11, 13].

Below we demonstrate that this single-impurity scenario breaks down in the case of the TAFM already at very small vacancy concentrations. We find analytically and numerically that in magnetic field impurities favor the *least* collinear state, *i.e.*, the non-coplanar conical or umbrella spin structure, Fig. 1(d). The behavior of the diluted TAFM is, therefore, strongly affected by competition between quenched and thermal disorder. The phase diagram of a diluted classical TAFM provides a

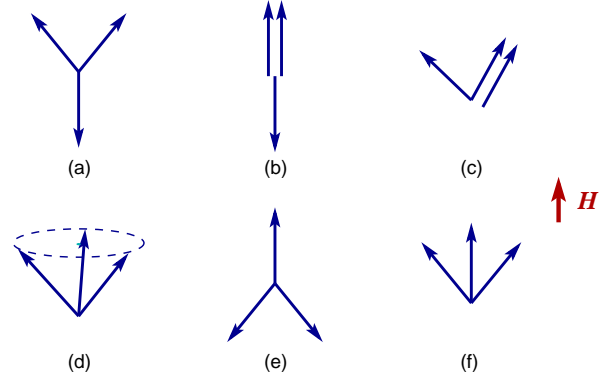


FIG. 1. (Color online) Ordered magnetic states of a TAFM in an external field. Spin configurations appearing for the TAFM without impurities: (a) coplanar Y-state, (b) collinear *uud* state, and (c) coplanar 2:1 (V) state. Spin configurations in the presence of nonmagnetic impurities: (d) conical (umbrella) state of the Heisenberg TAFM, (e) ‘anti-Y’ state and equivalent (f) fan state of the XY TAFM.

rare physical example in which nonmagnetic impurities tune bulk properties of an ordered antiferromagnet and drastically modify its phase diagram.

Theory.—We consider the classical Heisenberg antiferromagnet on a depleted triangular lattice described by the spin Hamiltonian

$$\hat{\mathcal{H}} = J \sum_{\langle ij \rangle} p_i p_j \mathbf{S}_i \cdot \mathbf{S}_j - \mathbf{H} \cdot \sum_i p_i \mathbf{S}_i \quad (1)$$

with $|\mathbf{S}_i| = 1$ and $p_i = 1$ or 0 for filled and empty sites, respectively. The clean model with no depletion, $p_i \equiv 1$, orders at $T = 0$ in the 120° three-sublattice magnetic structure described by the wavevector $\mathbf{Q} = (4\pi/3, 0)$. In magnetic field the classical energy is minimized for spin configurations constrained by the magnetization of each triangular plaquette:

$$\mathbf{S}_\Delta = \mathbf{H}/(3J) . \quad (2)$$

The constraint leaves undetermined the orientation of the spin plane and sublattice directions inside that plane. This degeneracy persists up to the saturation field $H_s = 9J$.

An empty site produces a strong local perturbation in the 120° magnetic structure leading to readjustment of neighboring spins with a characteristic power-law decay with distance [11]. Therefore, for the sake of analytical analysis we resort to a simpler model of weak bond disorder: the lattice is assumed to be fully filled, whereas the exchange parameters J_{ij} fluctuate randomly about the mean value J with $\langle \delta J_{ij}^2 \rangle = \delta J^2$. The bond disorder may develop in magnets with sizeable magnetoelastic coupling. In our case, a transformation between the site-disorder model (1) and the bond-disorder model with $J_{ij} = Jp_i p_j$ can be constructed by (i) allowing $p_i \in (0, 1)$, *i.e.*, letting spins on impurity sites to change their length continuously, and (ii) assuming sufficient density of impurities such that coupling constants for adjacent bonds fluctuate independently. The latter condition is expected to be satisfied for $n_{\text{imp}} \gtrsim 3\text{--}5\%$ once a distance between impurities is not too large. Numerically, we find that the qualitative behavior obtained for the bond-disorder model remains valid for the site-dilution model (1) with the vacancy density as low as $n_{\text{imp}} \sim 0.1\%$.

To treat the effect of small thermal fluctuations $T \ll J$ and weak quenched disorder $\delta J \ll J$ on equal footing, we employ the real-space perturbation theory used for clean frustrated magnets in [25–27]. The starting point is an arbitrary ground-state spin configuration of the TAFM in external magnetic field. To take into account small fluctuations the Heisenberg Hamiltonian is transformed into the ‘rotating’ local frame with the z_i axis directed parallel to \mathbf{S}_i :

$$\hat{\mathcal{H}} = \sum_{\langle ij \rangle} J_{ij} [S_i^y S_j^y + \cos \theta_{ij} (S_i^z S_j^z + S_i^x S_j^x) + \sin \theta_{ij} (S_i^z S_j^x - S_i^x S_j^z)] - \mathbf{H} \cdot \sum_i \mathbf{S}_i. \quad (3)$$

Here and below S_i^α denote spin components in the local frame and θ_{ij} is an angle between two neighboring spins. Terms containing only S_i^z and/or S_j^z provide the classical energy and the mean-field fluctuations of spins in a local magnetic field. By analogy to other frustrated models [26, 27], one can show that a local field for the TAFM is the same on every site $H_{\text{loc}} = 3J$ irrespective of $H \leq H_s$. Consequently, the local mean-field fluctuations are governed by the Hamiltonian

$$\hat{\mathcal{H}}_0 = -H_{\text{loc}} \sum_i S_i^z \simeq \frac{H_{\text{loc}}}{2} \sum_i [(S_i^x)^2 + (S_i^y)^2], \quad (4)$$

where we expanded $S_i^z = \sqrt{1 - (S_i^x)^2 - (S_i^y)^2}$ and use \simeq to indicate that a constant is dropped in the final expression.

In the absence of random disorder ($J_{ij} \equiv J$) the terms linear in S_i^x sum up to zero for all classical ground states. Then, the perturbation to Eq. (4) is

$$\hat{V}_1 = J \sum_{\langle ij \rangle} (S_i^y S_j^y + S_i^x S_j^x \cos \theta_{ij}). \quad (5)$$

The leading correction to the free-energy is given by $\Delta F = -\langle \hat{V}_1^2 \rangle / 2T$. Using $\langle (S_i^x)^2 \rangle = \langle (S_i^y)^2 \rangle = T/H_{\text{loc}}$ derived from Eq. (4), we obtain

$$\Delta F = -\frac{J^2 T}{2H_{\text{loc}}^2} \sum_{\langle ij \rangle} (\cos^2 \theta_{ij} + 1) \simeq -\frac{T}{18} \sum_{\langle ij \rangle} (\mathbf{S}_i \cdot \mathbf{S}_j)^2, \quad (6)$$

where in the last expression we restore the mean-field (ground-state) spin directions. Thus, short-wavelength thermal fluctuations produce an effective biquadratic exchange. Quantum fluctuations also generate a similar term [26]. Due to its negative sign, the biquadratic exchange (6) favors the ‘most collinear’ spin configurations among degenerate classical states. For the TAFM this leads to selection of the coplanar configurations, Figs. 1(a) and 1(c), at low and high fields, respectively, and to appearance of the $1/3$ magnetization plateau with the collinear up-up-down (*uud*) spin structure, Fig. 1(b).

We now set $T = 0$ and consider the effect of quenched disorder, which locally violates the perfect geometrical frustration. In this case the linear terms provide the main perturbation to the classical energy:

$$\hat{V}_2 = \sum_{\langle ij \rangle} \delta J_{ij} \sin \theta_{ij} (S_j^x - S_i^x). \quad (7)$$

Minimization of $\hat{\mathcal{H}}_0 + \hat{V}_2$ with respect to S_i^x under the assumption that bonds fluctuate independently yields

$$\Delta E = -\frac{\delta J^2}{2H_{\text{loc}}} \sum_{i,j} \sin^2 \theta_{ij} \simeq \frac{\delta J^2}{3J} \sum_{\langle ij \rangle} (\mathbf{S}_i \cdot \mathbf{S}_j)^2, \quad (8)$$

The energy correction generated by the bond disorder has the same functional form as (6) but with the opposite sign. Therefore, the configurational disorder favors the ‘least collinear’ states in the ensemble of degenerate classical ground states. Selection of orthogonal or ‘anticollinear’ ground states was previously known in the context of the diluted J_1 – J_2 square-lattice antiferromagnet [12, 16] yet the tendency determined by (8) is rather general, see also Refs. [28, 29] with similar conclusions.

In the case of the Heisenberg TAFM in an external field the ‘least collinear’ state corresponds to the conical spin structure, Fig. 1(d). Thus, the two types of disorder, thermal and quenched, compete with each other producing a rich H – T phase diagram. Note that Eqs. (6) and (8) are only approximate and constitute the first terms in the $1/z$ expansion, z being the number of the nearest neighbors [29]. Still, as comparison with the numerics

shows, the effective biquadratic exchange is able to capture the principal qualitative tendencies for the TAFM.

Ground state selection.—To extend the qualitative analytical result obtained for the weak bond disorder to the case of random vacancies we performed numerical minimization of the classical energy (1). The minimization is carried out for periodic $L \times L$ clusters with fixed concentration of nonmagnetic impurities $n_{\text{imp}} = 0.1\text{--}5\%$ and linear sizes up to $L = 150$. One starts with a random spin configuration and solves iteratively the local minimum condition $\mathbf{S}_i^{(k)} \parallel \mathbf{h}_i^{(k)}$, where the local field is $\mathbf{h}_i^{(k)} = \mathbf{H} - J \sum_j p_j \mathbf{S}_j^{(k-1)}$. Once converged the procedure is repeated with up to 10^3 random initial configurations and the global minimum is selected. Physical quantities are then averaged over 100 impurity replicas.

Ground-state configurations of the TAFM in magnetic field are characterized by the antiferromagnetic order parameter:

$$\mathbf{M}_Q = \frac{1}{N} \sum_i \mathbf{S}_i e^{-i\mathbf{Q}\cdot\mathbf{r}_i} \quad (9)$$

with N being the number of filled sites. In particular, the conical state is unambiguously distinguished from the coplanar configurations by a finite $M_Q^\perp = (|M_Q^x|^2 + |M_Q^y|^2)^{1/2}$ and $|M_Q^z| = 0$.

Numerical results for transverse and longitudinal components of the AFM order parameter at $H/J = 3$ are shown in Fig. 2. The conical state remains stable for all studied impurity concentrations including the smallest one $n_{\text{imp}} = 0.1\%$. The lack of appreciable finite-size effects in M_Q^\perp indicates the absence of a spin-glass phase and the development of the true long-range order in transverse components. A similar behavior is found for all $0 < H < H_s$ albeit with more iteration steps required for $H \rightarrow 0$. Hence, the numerical results for the diluted TAFM fully corroborate the analytical findings for the bond-disorder model. The vacancy moment effect [11, 13] averages to zero due to equal occupation of magnetic sublattices by impurities and the finite-field behavior is determined by configurational fluctuations which are correctly captured by the bond-disorder model.

Phase diagram.—We have performed the classical Monte Carlo (MC) simulations of the diluted TAFM in a wide range of temperatures and magnetic fields using the hybrid algorithm, which combines the Metropolis step with a few overrelaxation moves, see [30, 31] for further details. Physical quantities and associated error bars were estimated from averaging over 100 impurity replicas. Phase transition boundaries were determined by the standard finite-size scaling analysis of the fourth-order Binder cumulants for the AFM order parameter (9) and the associated spin chirality, as well as from the behavior of the spin stiffness and the specific heat on clusters with linear sizes up to $L = 150$.

The magnetic phase diagram of the Heisenberg TAFM

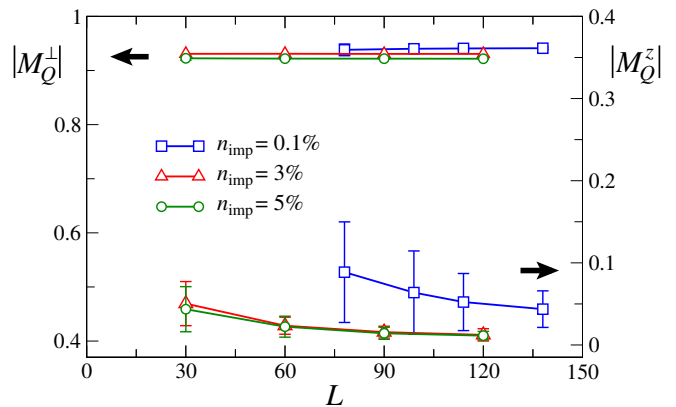


FIG. 2. (Color online) Zero-temperature transverse $|M_Q^\perp|$ and longitudinal $|M_Q^z|$ antiferromagnetic order parameters at $H/J = 3$ for clusters with different concentration of vacancies n_{imp} and different linear size L .

with 5% of vacancies is shown in Fig. 3. The main new feature in comparison with the diagram of the pure model [19, 31, 32] is the emergence of the conical state at low temperatures for all $H \leq H_s$. At high enough temperatures the increased thermal fluctuations overcome the quenched disorder and magnetic phases of the pure TAFM reappear again, though the Y-phase remains absent for $n_{\text{imp}} = 5\%$. The phase transition boundaries are drawn in Fig. 3 down to $H/J \sim 1$. In lower magnetic fields, the finite-size effects become stronger and require simulations of significantly larger clusters than those studied in our work. Therefore, we cannot exclude reappearance of the Y-phase at very low fields. Instead we show evolution of the phase boundaries with the vacancy concentration at fixed $H = 1.3J$ in the inset of

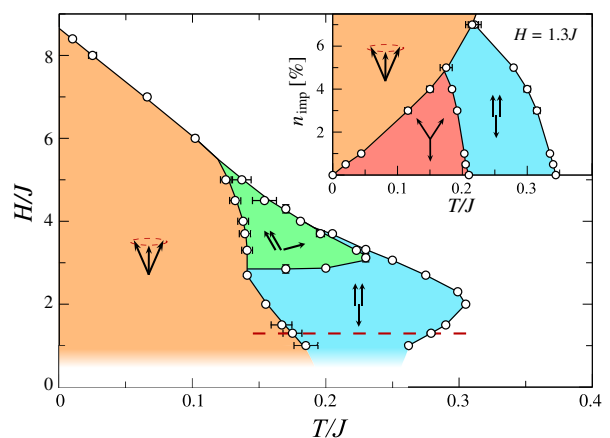


FIG. 3. (Color online) Classical Monte Carlo phase diagram of the Heisenberg TAFM with 5% of nonmagnetic impurities. Solid lines via data points are guides for the eye. The inset shows the concentration evolution of ordered phases for $H/J = 1.3$, which is indicated by the dashed line on the main panel.

Fig. 3. The Y-phase is present in this field for small n_{imp} and disappears at $n_{\text{imp}} \sim 4.5\%$.

The effect of impurities on the critical behavior of the TAFM can be assessed using the Harris criterion [33], which states that the disorder becomes relevant for transitions with $\alpha = 2 - d\nu > 0$. In particular, the Berezinskii-Kosterlitz-Thouless (BKT) transition formally has $\nu = \infty$ and remains unaffected by vacancies as was confirmed numerically in [34]. The second-order transition into the *uud* state, which belongs to the universality class of the 2D three-state Potts model, has $\alpha = 1/3$ and is, therefore, driven by impurities to a new random fixed point, see [35, 36] and references therein. Nevertheless, the spin correlation exponent η stays very close to the clean value $\eta = 4/15$ [35] and we also found virtually no difference with the pure case for the critical behavior of the order parameter at this transition in our Monte Carlo simulations.

In the high-field region $5J \lesssim H < H_s$ the direct transition between paramagnetic and conical states is accompanied by breaking of the $\mathbb{Z}_2 \otimes O(2)$ symmetry, where \mathbb{Z}_2 describes the chirality ordering. The statistical errors in simulations brought by the impurities are too large to resolve a presumably tiny splitting of T_{BKT} and T_{chir} as well as an effect of the disorder on the Ising-like chiral transition. Finally, transitions between coplanar states and the conical phase are expected to be of the first-order on symmetry grounds. Indeed, there is a signature of the first-order transition for $2J \lesssim H < 3J$ from the scaling of the specific heat anomaly. At higher and lower fields the diluted TAFM shows fingerprints of a continuous transition between conical and coplanar states, which may also signify presence of an intermediate phase in a narrow temperature interval.

XY triangular antiferromagnet.—Let us now briefly discuss the effect of nonmagnetic impurities in the easy-plane TAFM—model relevant to a number of real materials. Some of them exhibit the $1/3$ magnetization plateau for fields applied parallel to the easy plane [24, 37], which is a clear sign of geometrical magnetic frustration. The ordered states of the XY TAFM in the presence of an in-plane magnetic field were investigated by Lee *et al.* [18]. Thermal fluctuations lift the ground-state degeneracy in favor of the same sequence of phases in magnetic field as for the Heisenberg model, see Fig. 1(a)–(c). Our derivation of an effective biquadratic exchange for the weak bond disorder remains intact for the XY spins. Hence, the only difference with the isotropic case is that the conical state, Fig. 1(d), as well as other non-coplanar configurations are now forbidden. Therefore, the biquadratic exchange (8) lifts the degeneracy between the coplanar structures only. An elementary analysis shows that the lowest energy state favored by a positive biquadratic exchange corresponds to the ‘anti-Y’ spin configuration shown in Fig. 1(e). In stronger magnetic fields the two canted spins tilt further towards the field direction con-

tinuously transforming the ‘anti-Y’ state into the ‘fan’ spin structure, Fig. 1(f).

We have complemented analytical consideration with numerical search for the lowest-energy magnetic structures using the same technique as for the isotropic model. Numerical results, which will be reported elsewhere [38], are fully consistent with the presence of the fan (anti-Y) state in the whole range of magnetic fields. Interestingly, a new high-field state interpreted as a fan structure was recently observed in the easy-plane spin-1/2 TAFM $\text{Ba}_3\text{CoSb}_2\text{O}_9$ [37]. Though, the full theoretical explanation of the new phase should include quantum effects, our analysis of the classical model suggests that nonmagnetic impurities may play a key role in its appearance.

Discussion.—Nonmagnetic impurities modify the behavior of the classical TAFM in an external magnetic field. The effect of static disorder can be qualitatively described by a positive biquadratic exchange, which competes with a similar effective interaction of the opposite sign generated by thermal and quantum fluctuations. At zero temperature vacancies stabilize the conical state for the Heisenberg TAFM, whereas for the XY model with an in-plane field they favor the fan-like spin structure. A similar competition between the quenched disorder and thermal effects must also be present in other geometrically frustrated antiferromagnets.

Beyond the classical model, quantum fluctuations will compete with the effect of dilution even at $T = 0$. For a given spin value S , there is a critical concentration of vacancies $n_{\text{imp}}^c \sim 1/S$ needed to overcome the quantum selection of ‘most collinear’ states. Comparing the harmonic spin-wave energies of the *uud* and conical states [20] with the classical energy gain of the conical state obtained from the numerical minimization we find that the $1/3$ magnetization plateau of the Heisenberg TAFM is stable up to $n_{\text{imp}}^c \sim 4\%$ for $S = 5/2$ [38]. This estimate for n_{imp}^c becomes even lower once quantum effects are further suppressed by weak magnetic anisotropy. Systematic experimental studies of frustrated magnets doped with nonmagnetic impurities may, therefore, bring new fascinating physics. Apart from the fundamental interest, this can open additional possibilities in controlling electrical and magnetic polarizations in triangular multiferroics.

We acknowledge helpful discussions with A. L. Chernyshev and M. Vojta.

-
- [1] O. P. Vajk, P. K. Mang, M. Greven, P. M. Gehring, and J. W. Lynn, *Science* **295**, 1691 (2002).
 - [2] J. Bobroff *et al.*, *Phys. Rev. Lett.* **103**, 047201 (2009).
 - [3] M. Sigrist and A. Furusaki, *J. Phys. Soc. Jpn.* **65**, 2385 (1996).
 - [4] S. Sachdev, C. Buragohain, and M. Vojta, *Science* **286**, 2479 (1999).

- [5] S. Sachdev and M. Vojta, Phys. Rev. B **68**, 064419 (2003).
- [6] O. P. Sushkov, Phys. Rev. B **68**, 094426 (2003).
- [7] K. H. Höglund, A. W. Sandvik, and S. Sachdev, Phys. Rev. Lett. **98**, 087203 (2007).
- [8] S. Eggert, O. F. Syljuåsen, F. Anfuso, and M. Anders, Phys. Rev. Lett. **99**, 097204 (2007).
- [9] C.-C. Chen, R. Applegate, B. Moritz, T. P. Devereaux, and R. R. P. Singh, New J. Phys. **13**, 043025 (2011).
- [10] A. Sen, K. Damle, and R. Moessner, Phys. Rev. Lett. **106**, 127203 (2011).
- [11] A. Wollny, L. Fritz, and M. Vojta, Phys. Rev. Lett. **107**, 137204 (2011).
- [12] C. Weber and F. Mila, Phys. Rev. B **86**, 184432 (2012).
- [13] A. Wollny, E. C. Andrade, and M. Vojta, Phys. Rev. Lett. **109**, 177203 (2012).
- [14] W. Brenig and A. L. Chernyshev, Phys. Rev. Lett. **110**, 157203 (2013).
- [15] J. Villain, Z. Phys. B **33**, 31 (1979).
- [16] C. L. Henley, Phys. Rev. Lett. **62**, 2056 (1989).
- [17] L. Savary, E. Gull, S. Trebst, J. Alicea, D. Bergman, and L. Balents, Phys. Rev. B **84**, 064438 (2011).
- [18] D. H. Lee, J. D. Joannopoulos, J. W. Negele, and D. P. Landau, Phys. Rev. Lett. **52**, 433 (1984).
- [19] H. Kawamura and S. Miyashita, J. Phys. Soc. Jpn. **54**, 4530 (1985).
- [20] A. V. Chubukov and D. I. Golosov, J. Phys. Condens. Matter **3**, 69 (1991).
- [21] L. Balents, Nature **464**, 199 (2010).
- [22] J. Struck *et al.*, Science **333**, 996 (2011).
- [23] T. Katsufuji, S. Mori, M. Masaki, Y. Moritomo, N. Yamamoto, and H. Takagi, Phys. Rev. B **64**, 104419 (2001).
- [24] M. Kenzelmann *et al.*, Phys. Rev. Lett. **98**, 267205 (2007).
- [25] M. W. Long, J. Phys.: Condens. Matter **1**, 2857 (1989).
- [26] M. T. Heinilä and A. S. Oja, Phys. Rev. B **48**, 7227 (1993).
- [27] B. Canals and M. E. Zhitomirsky, J. Phys.: Condens. Matter **16**, S759 (2004).
- [28] Y. V. Fyodorov and E. F. Shender, J. Phys.: Condens. Matter **3**, 9123 (1991).
- [29] B. E. Larson and C. L. Henley, arXiv:0811.0955 (unpublished).
- [30] M. E. Zhitomirsky, Phys. Rev. B **78**, 094423 (2008).
- [31] M. V. Gvozdkova, P.-E. Melchy, and M. E. Zhitomirsky, J. Phys.: Condens. Mat. **23**, 164209 (2011).
- [32] L. Seabra, T. Momoi, P. Sindzingre, and N. Shannon, Phys. Rev. B **84**, 214418 (2011).
- [33] A. B. Harris, J. Phys. C **7**, 1671 (1974).
- [34] B. Berche, A. I. Farinas-Sanchez, Yu. Holovatch, and R. Paredes V., Eur. Phys. J. B **36**, 91 (2003).
- [35] J.-K. Kim, Phys. Rev. B **53**, 3388 (1996).
- [36] M. Picco, Phys. Rev. B **54**, 14930 (1996).
- [37] T. Susuki *et al.*, Phys. Rev. Lett. **110**, 267201 (2013).
- [38] V. S. Maryasin and M. E. Zhitomirsky, to be published.